Send Orders for Reprints to reprints@benthamscience.ae

The Open Automation and Control Systems Journal, 2015, *7*, 157-166

Open Access

Application of a PID-GPC Algorithm in a Ball-Mill System

Sun Lingfang[1,*], Sun Jingmiao[1], Miao Yinde[2], Fu Congwei[2], Ren Jibing[2] and Yu Wei[3]

[1]*School of Automation Engineering, Northeast Dianli University, Jilin, 132012, China*

[2]*Shandong Huaju Energy Co., LTD, Zoucheng, Shandong, 273500, China*

[3]*China Huadian Electric Power Research Institute, Hangzhou, Zejiang, 310030, China*

Abstract: A direct-fired pulverizing system with double inlets and outlets, as an important power generating plant in thermal power stations, is characterized by non-linear, multivariable, strong coupling and a large delay. Meanwhile, a ball-mill is a typical three-input, three-output system: how to model this system and accomplish its automatic control has become a hot spot in today's research on thermal power generation. This paper takes into account PID control, the most widely used basic control law in industrial process control, and based on the generalized predictive control algorithm, applies the proportional integral differential structured generalized predictive control algorithm (PID-GPC) to the ball-mill. This algorithm incorporates the advantages of the robustness and predictive control model of the traditional PID control algorithm. The simulation of a 300 MW power unit ball-mill pulverizing system running under a negative pressure in a given power plant in Longshan, Hebei Province shows that such an algorithm offers better robustness than general feed-forward decoupling PID control and GPC control: it is also more suited to industrial application.

Key words: Automatic control, ball-mill, control method, generalized predictive control.

1. INTRODUCTION

A ball-mill, as important item of equipment in coal preparation systems, is widely used in large-scale thermal power plants both at home and abroad [1]. Currently, there are two major types of ball-mills using in utility boilers: single inlet and outlet, double inlet and outlet ball-mills. As the ball-mill represents a non-linear process which is characterized by a large delay and many uncertain external influences, it is difficult to establish a precise mathematical model thereof. Meanwhile, the ball-mill is a typical three-input, three-output system, and for such a high-level, strongly-coupled, non-linear system, how to model this system and accomplish its automatic control has become a hot spot in today's research into thermal power generation.

Traditional PID control still plays an important role in practical industrial applications due to such characteristics as simplicity in principle, robustness, and ease of implementation. However, in industrial process control, the non-linearity, large delay, and object model parameters may change as the working parameters change, and there are many other factors beyond human control. Therefore, with a separate PID control algorithm it is difficult to achieve a satisfactory control effect.

Engineers are no longer satisfied with traditional stabilisation design. Instead, they demand better performance by control system optimisation [2]. The theory of predictive control developed in the late 1970s is a control algorithm that is based on the predictive process model. Due to its successful application in generalised predictive control algorithms, research into improvements to this algorithm is also flourishing. Here, as elsewhere [3], the PID controller has a time-varying proportional gain, and the PID parameters are designed using the future reference trajectory of the GPC. Others [4,5] have proposed a new PID tuning scheme (GPC-PID) which is derived from the relationship between the GPC and the PID control laws as proposed in this paper. Furthermore, the implementation of GPC-PID for existing PID auto-tuners is considered. Others [6-8] have proposed a PI-GPC scheme, since the design parameters of GPC are selected to achieve user-specified control performance: the PI parameters are adaptively updated such that the control performance is improved. In the proposed method, the estimated plant parameters of a weigh-feeder are updated only when the estimation error increases. Therefore, the control system is not updated frequently, and the control system is updated only when the control performance is sufficiently improved. Combining the structure of the PID with a GPC algorithm, and combining the structure of the PI and GPC algorithms can enhance the robustness, and render the system suitable for industrial application. Generalised predictive control [9] seems to be an attractive solution in process control, especially for multivariable systems.

This paper mainly deals with double inlet and outlet ball-mill systems, establishes a mathematical model in the light of a least-squares method, and according to step-output curve of the transfer function model, obtains the object model parameters of the ball-mill through identification. Since the PID method is still widely used, through the improvement of the generalized predictive control algorithm, and by combining PID control with GPC control, we applied a pro-

*Address correspondence to this author at Changchun Road 169 Northeast Dianli University, Jilin, 132012, China; Tel: 15043283452;
E-mail: dr_sunlf@163.com

1874-4443/15

portional integral differential structured generalized predictive self-tuning controller (PID-GPC) to the mathematical model of the ball-mill. By MATLAB™ simulation, we compared this algorithm with the PID control algorithm (based on feed-forward compensation decoupling) and verified the superiority of this algorithm.

2. WORKING PRINCIPLE BEHIND A BALL-MILL

A double inlet and outlet ball-mill has two perfectly symmetrical powder loops [10]. It works as follows: raw coal falls from the coal bucket, passes through the coal chute, and is mixed with hot air. After the raw coal is dried, it enters the coal pulveriser and is crushed. The pulverized coal will then be carried by the hot air to the air separator at the top of the mill. The pulverized powder will be mixed with an air-drying medium, forming a coal-air mixture which will enter, through the pulverized coal pipeline, the combustion chamber for combustion [11]. The disqualified pulverized powder will return to the coal pulveriser for re-milling. Actually, a ball-mill is a non-linear system characterized by multivariable, large delay, strong coupling and slow time-variation.

3. MATHEMATICAL MODEL OF A DOUBLE INLET AND OUTLET BALL-MILL

3.1. The Least Squares Method Applied to the Step-Response Identification

For SISO discrete stochastic systems:

$$y(k) = -a_1 y(k-1) - \cdots - a_{n_a} y(k-1) + b_1 x(k-1) + b_2 x(k-2) + \cdots + b_{n_b} x(k-n_b) + e(k) \quad (1)$$

In Eq. (1): $y(k)$ is the K-th observed value of system outputs, $y(k-1)$ is the k-1-th observed value of system outputs, and so on; $x(k)$ is the K-th input value of system, $x(k-1)$ is the k-1-th input value of the system; $e(k)$ is random noise (zero mean).

System input and output least squares are:

$$y(k) = h^T(k)\theta + e(k) \quad (2)$$

In (2): h is a sample set, θ is a set of identified parameters.

$$\begin{cases} h(k) = [-y(k-1), \cdots, -y(k-n_a), x(k-1), \cdots, x(k-n_b)]^T \\ \theta = [a_1, a_2 \cdots, a_{n_a}, b_1, b_2 \cdots, b_{n_b}]^T \end{cases}$$

Take the criterion function:

$$J(\theta) = \sum_{k=1}^{\infty} [e(k)]^2 = \sum_{k=1}^{\infty} [y(k) - h^T(k)\theta]^2 \quad (3)$$

The estimated value of θ for $J(\theta) = \min$ is denoted as $\hat{\theta}_{LS}$, which is the least-squares estimate of parameter θ.

The basic concept above suggests that the most possible value of the unknown model parameter θ is the minimum sum of squares of iterated errors between the actual observed, and calculated, values. Such output from the model thus derived can be the most approximate to the actual output of the system.

3.2. To Determine the Parameters of Delayed First-Order Inertia by the Step-Response Curve

This paper, by using the least squares fitting method, obtains the approximate model of the actual object with minimum deviation in accordance with the soaring curve of such objects. Fig. (**1**) shows a schematic block diagram of the method for obtaining the object model.

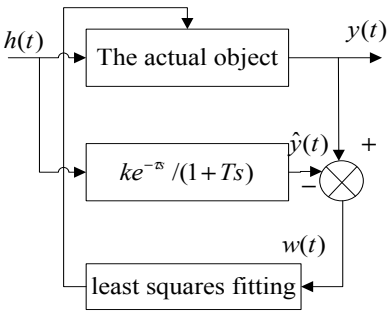

Fig. (1). Block diagram of the method for obtaining the model.

In the formula, *h* is a unit step signal see Fig. (**1**),

$$y(t) = \hat{y}(t) + w(t) \quad (4)$$

In the formula: $y(t)$ is the output of the actual object. $\hat{y}(t)$ is the output of the approximate model.

Provided $\hat{G}(s) = ke^{-\tau s}/(1+Ts)$,

Then
$$\hat{y}(t) = \begin{cases} 0 & (\forall t < \tau) \\ k(1 - e^{-(t-\tau)T}) & (\forall t \geq \tau) \end{cases} \quad (5)$$

$$y(t) = \hat{y}(t) + w(t) = \begin{cases} w(t) & (\forall t < \tau) \\ k(1 - e^{-(t-\tau)T}) + w(t) & (\forall t \geq \tau) \end{cases} \quad (6)$$

It is derived from Eq. (6):

$$e^{-(t-\tau)T} = 1 - \frac{y(t)}{k} + \frac{w(t)}{k}, (\forall t \geq \tau) \quad (7)$$

Integrating (6) on both sides and substituting (7), gives (upon rearrangement):

$$\int_0^l y(t)dt = hk[l - \tau - \frac{Ty(l)}{k}] + [Tw(l)]|_\tau^l + \int_0^l w(t)dt, (\forall l \geq \tau) \quad (8)$$

Provided

$$A(l) = \int_0^l y(t)dt, \delta(l) = [Tw(l)]|_\tau^l + \int_0^l w(t)dt$$

Eq. (8) can be rewritten as:

$$A(l) = k[l - \tau - \frac{Yy(l)}{k}] + \delta(l), (\forall l \geq \tau) \quad (9)$$

The Eq. (9) is written in least-squares format:

$$A(l)=[l \quad -1 \quad -y(l)]\begin{bmatrix} k \\ \tau k \\ T \end{bmatrix}+\delta(l),(\forall l \geq \tau) \tag{10}$$

Provided that $\theta=[k \quad \tau k \quad T]^T$,

$$A_l=\begin{bmatrix} A(mT_s) \\ A((m+1)T_s) \\ \cdots \\ A((m+n)T_s) \end{bmatrix}, \quad \delta_l=\begin{bmatrix} \delta(mT_s) \\ \delta((m+1)T_s) \\ \cdots \\ \delta((m+n)T_s) \end{bmatrix}$$

$$H_l=\begin{bmatrix} mT_s & -1 & -y(mT_s) \\ (m+1)T & -1 & -y((m+1)T_s) \\ \cdots & & \\ (m+n)T_s & -1 & -y((m+n)T_s) \end{bmatrix}.$$

By the least squares method, the least squares are estimated as $\hat{\theta}=(H_L^T H_L)^{-1} H_L^T A_L$, and k, T, τ can be obtained from Eq. (10).

4. PID-TYPE GENERALISED PREDICTIVE CONTROL ALGORITHM (PID-GPC) PRINCIPLE

The Generalized Predictive Control algorithm is a predictive control algorithm developed from much research into adaptive control. It has not only absorbed the adaptive control that applied to stochastic systems, on-line identification, and other advantages, but also maintained the rolling optimization strategy in the predictive control algorithm, and the advantages of less precision for the model.

Consider the following CARIMA model:

$$A(z^{-1})y(k)=B(z^{-1})u(k-1)+\frac{C(z^{-1})\xi(k)}{\Delta} \tag{11}$$

Where

$$A(z^{-1})=1+a_1 z^{-1}+\cdots+a_{n_a} z^{-n_a}, \deg A(z^{-1})=n_a$$

$$B(z^{-1})=b_0+b_1 z^{-1}+\cdots+b_{n_b} z^{-n_b}, \deg B(z^{-1})=n_b$$

$$C(z^{-1})=c_0+c_1 z^{-1}+\cdots+c_{n_c} z^{-n_c}, \deg C(z^{-1})=n_c$$

where $A(z^{-1})$, $B(z^{-1})$ and $C(z^{-1})$ are z^{-1} polynomials for n, m, and n-level cases; z^{-1} is a back-forward shift operator; $\Delta=1-z^{-1}$ is a difference operator; $\xi(k)$ is a white noise sequence with zero mean. This article ignores the effects of white noise.

The objective function on which the PID-GPC is based is:

$$J=\{E\sum_{j=1}^{n}[K_p(e(k+j))^2+K_i(\Delta e(k+j))^2 + K_d(\Delta^2 e(k+j))^2]+\lambda\sum_{j=1}^{m}[(\Delta u(k+j-1)]^2\} \tag{12}$$

Where, $e(k+j)=\Delta e(k+j)=0$; n——Before predicted bits; m——Before control bits; λ——Control weighting constant factor; $K_p \geq 0$ is a coefficient of proportionality; $K_i > 0$ is an integration coefficient; $K_d > 0$ is a differential coefficient.

$$e(k+j)=\Delta e(k+j)-\Delta e(k+j-1)$$
$$j=1,\cdots,N_y \tag{13}$$

According to theoretical predictions, to predict the forward j-step output, the following Diophantine equation is introduced:

$$C(z^{-1})=E_j(z^{-1})A(z^{-1})\Delta+z^{-j}F_j(z^{-1})$$
$$j=1,\cdots,N_y \tag{14}$$

$$E_j(z^{-1})B(z^{-1})=G_j(z^{-1})C(z^{-1})\Delta+z^{-j}H_j(z^{-1})$$
$$j=1,\cdots,N_y \tag{15}$$

Where, $E_j(z^{-1})$——j-1 times to be polynomial; $F_j(z^{-1})$——N_a times to be polynomial; the order of H_j is $\max(n_b-1,n_c-1)$.

The following predictive equation can be obtained from Eqs (11), (14), and (15):

$$y(k+j)=H_j\Delta u'(k+j)+E_j D\Delta v'(k+j-1)+F_j y'(k)+G_j\Delta u'(k+j-1)+E_j\xi(k+j)$$
$$j=1,\cdots,N \tag{16}$$

Where, $y'(k)=y(k)/C(z^{-1})$; $u'(k)=u(k)/C(z^{-1})$; $v'(k)=v(k)/C(z^{-1})$; $v'(k)=v(k)/C(z^{-1})$

Defined as:

$$f(k+j)=F_j y'(k)+H_j\Delta u'(k-1)+E_j D\Delta v'(k+1-j) \tag{17}$$

Eq. (16) can be abbreviated to:

$$y(k+j)=f(k+j)+G_j\Delta u'(k+j-1)+E_j\xi(k+j) \tag{18}$$

According to Eq. (18), we obtain the optimal forward output forecast of the j-th step:

$$\bar{y}(k+j\,|\,k)=f(k+j)+G_j\Delta u(k+j-1) \tag{19}$$

Thus

$$e(k+j)=[w(k+j)-f(k+j)]-G_j\Delta u(k+j-1)-E_j\xi(k+j) \tag{20}$$

$$\Delta e(k+j)=[\Delta w(k+j)-\Delta f(k+j)]-G_j\Delta u(k+j-1)-E_j\xi(k+j) \tag{21}$$

$$\Delta^2 e(k+j)=[\Delta^2 w(k+j)-\Delta^2 f(k+j)]-G_j\Delta u(k+j-1)-E_j\xi(k+j) \tag{22}$$

$w(k+j)$ is a set value sequence.

Because

$$e(k)=w(k)-y(k)=0$$
$$\Delta e(k+j)=[\Delta w(k+j)-\Delta f(k+j)]-$$
$$[G_j\Delta u(k+j-1)-G_j-\Delta u(k+j-2)]-$$
$$[E_j\xi(k+j)-E_j-\xi(k+j-1)] \quad (23)$$

Provided

$$\Delta e(k+1)=e(k+1)-e(k)=e(k+1) \quad (24)$$

In addition, provided that

$$\overline{w}=[w(k+1),\cdots,w(k+N_y)]^T$$
$$\Delta\overline{w}=[w(k+1),\Delta w(k+1),\cdots,w(k+N_y)]^T$$
$$\Delta^2\overline{w}=[w(k+1),\Delta w(k+1),\cdots,\Delta^2 w(k+N_y)]^T$$
$$\bar{f}=[f(k+1),f(k+2),\cdots,f(k+N_y)]^T$$
$$\Delta\bar{f}=[f(k+1),f(k+2),\cdots,f(k+N_y)]^T$$
$$\Delta^2\bar{f}=[f(k+1),\Delta f(k+2),\cdots,\Delta^2 f(k+N_y)]^T$$
$$e=[e(k+1),\cdots,e(k+N_y)]^T$$
$$\Delta e=[e(k+1),\Delta e(k+2),\cdots,\Delta e(k+N_y)]^T$$
$$\Delta^2 e=[e(k+1),\Delta e(k+2),\Delta^2 e(k+3),\cdots,$$
$$\Delta^2 e(k+N_y)]^T$$
$$\bar{\xi}=[E_1\xi(k+1),E_2\xi(k+2)-E_1\xi(k+1),\cdots,$$
$$E_{N_y}\xi(k+N_y)-E_{N_{y-1}}\xi(k+N_y-1)]^T$$
$$\bar{u}=[\Delta u(k),\cdots,\Delta u(k+N_u-1)]^T \quad (25)$$

Where, g_i is the coefficient of $G_N(z^{-1})$ for z^{-1}.

When $j\geq N_u$, $\Delta u(k+j)=0$,

So, we can get

$$\bar{e}=\overline{w}-\bar{f}-G_i\bar{u}-\Delta\bar{\xi} \quad (26)$$

$$\Delta\bar{e}=\Delta\overline{w}-\Delta\bar{f}-G_P\bar{u}-\Delta\bar{\xi} \quad (27)$$

$$\Delta^2\bar{e}=\Delta^2\overline{w}-\Delta^2\bar{f}-G_d\bar{u}-\Delta^2\bar{\xi} \quad (28)$$

The objective function (2) can be sorted as follows:

$$J=E\{K_P\Delta\bar{e}^T\Delta\bar{e}+K_i\Delta\bar{e}^T\Delta\bar{e}+K_d\Delta^2\bar{e}^T\Delta\bar{e}+\lambda\Delta\bar{u}^T\Delta u\} \quad (29)$$

Upon optimizing control sequences, we can get:

$$\bar{u}=[\lambda I+K_p{G_p}^TG_p+K_i{G_i}^TG_i+K_d{G_d}^TG_d]^{-1}$$
$$[K_p{G_p}^T(\Delta\overline{w}-\Delta\bar{f})+K_i{G_i}^T(\overline{w}-\bar{f})+K_d{G_d}^T(\Delta^2\overline{w}-\Delta^2\bar{f})] \quad (30)$$

In the above formula, provided that $K=[1,0,\cdots,0]^T$, taking the first line of the above equation, gives:

$$\Delta u(k)=K^T[\lambda I+K_p{G_p}^TG_p+K_i{G_i}^TG_i+K_d{G_d}^TG_d]^{-1}$$
$$[K_p{G_p}^T(\Delta\overline{w}-\Delta\bar{f})+K_i{G_i}^T(\overline{w}-\bar{f})+K_d{G_d}^T(\overline{w}-\bar{f})] \quad (31)$$

So this improved proportional-integral generalized predictive control can be expressed as:

$$u(k)=u(k-1)+{R_p}^T(\Delta\overline{w}-\Delta\bar{f})+{R_i}^T(\overline{w}-\bar{f})+{R_d}^T(\overline{w}-\bar{f}) \quad (32)$$

Where,

$$R_p=K_pK^T[\lambda I+K_p{G_p}^TG_p+K_i{G_i}^TG_i+K_d{G_d}^TG_d]^{-1}{G_p}^T \quad (33)$$

$$R_i=K_iK^T[\lambda I+K_p{G_p}^TG_p+K_i{G_i}^TG_i+K_d{G_d}^TG_d]^{-1}{G_i}^T \quad (34)$$

$$R_d=K_dK^T[\lambda I+K_p{G_p}^TG_p+K_i{G_i}^TG_i+K_d{G_d}^TG_d]^{-1}{G_d}^T \quad (35)$$

The following describes the parameter identification used:

Given prediction model:

$$\hat{A}(z^{-1})\Delta y'(k)=\hat{B}(z^{-1})u'(k-1)+\hat{D}(z^{-1})\Delta v'(k-1) \quad (36)$$

Where, the coefficients of $\hat{A}$, $\hat{B}$, and $\hat{D}$ are obtained by identification, $\beta(k)$can be estimated by least squares method. The model parameters and data parameters are respectively denoted in vector form as:

$$\theta_K=[-\hat{a}_1,\cdots,-\hat{a}_{n_a},\hat{b}_0,\cdots,\hat{b}_{n_b},\hat{d}_0,\cdots,\hat{d}_{n_d}]^T \quad (37)$$

$$\phi(k)=[\Delta y'(k-1),\cdots,\Delta u'(k-1),\cdots,\Delta u'(k-1),\cdots]^T \quad (38)$$

The estimated parameter vector, by using a recursive least squares method, is:

$$\theta_K=\theta_{K-1}+\frac{P_{K-1}\phi(k)}{\beta(k)\phi^T(k)P_{K-1}\phi(k)}\varepsilon(k) \quad (39)$$

$$Q(k)=P_{K-1}-\frac{P_{K-1}\phi(k)\phi^T(k)P_{K-1}}{1+\phi^T(k)P_{K-1}\phi(k)} \quad (40)$$

Where,

$$\beta(k)=1-\frac{1}{N(k)} \quad (41)$$

$$N(k)=\{[\phi^T(k)P_{K-1}\phi(k)+1]/\varepsilon^2(k)\}\sigma(k) \quad (42)$$

$$\varepsilon(k)=\Delta y'(k)-\theta_{K-1}^T\phi(k) \quad (43)$$

If

$$[1/\beta(k)]trace[Q_K]\leq 0,$$

Then

$Q_K=[1/\beta(k)]Q_K$, otherwise $P_K=Q_K$

While

$\sigma(k)=N(k)\sigma_\varepsilon(k)$, $C>\alpha^2$.

Where, $\sigma_{\varepsilon}^{2}(k)$ is the variance of $\sigma(k)$, $trace[Q_K]$ is the trace of Q_K.

5. THE MATHEMATICAL MODEL OF A DOUBLE INLET, DOUBLE OUTLET, BALL-MILL

Ball-mill site processes are based on the actual changes in their equilibrium equations [12]. Due to the presence of double inlets and outlets, a ball-mill with two perfectly symmetrical powder loops, namely the input variables of hot air, cold air, and coal consumption being duplicated, means that, in turn, the output variable of outlet temperature, import and export of differential pressure, inlet air pressure are also duplicated. Here we assume that the ball-mill, in its dynamic and static equilibria, at the ends of the input, and output, have equal variables, so simplifying the modeling.

5.1. Ball-Mill Mathematical Model: Outlet Temperature

The outlet temperature of a ball-mill is affected by many factors, such as air volume, coal volume, specific heat of coal, and hot air and cold air volumes. According to the energy-balance, the following equation can be derived [13]:

$$\frac{d[(C_{gq}w_{gq}+C_m w_m)t_m]}{dt}=C_r G_r t_r - C_{tf}(G_r+G_l)t_m \tag{44}$$

$$+C_l G_l t_l + \frac{B_{gm}C_{gm}t_c}{3.6} - \frac{B_m C_m t_m}{3.6} + Q_o - Q_c$$

$$Q_0 = 41.57B_{gm}/3.6 = 11.55B_{gm} \tag{45}$$

$$Q_c = B_{gm}\Delta w \cdot C_w \cdot t_m / 3.6 \tag{46}$$

5.2. Mathematical Model of Inlet and Outlet Differential Pressure

The differential pressure across a ball-mill reflects the height of the coal feeding it, namely:

$$\frac{d\Delta P}{dt}=3(1+0.8\mu)vk_{\xi}(Q_2/Q_{20})^2(G_r+G_l)/V \tag{47}$$

$$Q_2=(G_r+G_l)/1.283*(273.15+t_m)/273.15+G_w/0.804 \tag{48}$$

5.3. Mathematical Model of Inlet Wind Pressure

The inlet wind pressure reflects the air volume passing through the ball-mill. From empirical equations:

$$\frac{dP_{in}}{dt}=R(t_m+273.15)k_{\xi}(Q_2/Q_{20})^2/V \tag{49}$$

5.4. Test Modeling Simulation

To determine the dynamic characteristics of the model, we have to apply a certain amount of disturbance to the double inlet, double outlet, ball-mill, in the form of a step disturbance test for the above model, and establish the transfer function of the system model. Wherein, *P* represents the inlet suction, and *T* represents the outlet temperature. To determine the dynamic characteristics of the model, we add a certain amount of disturbance to each input variable (*i.e.* to the amount of cold air, hot air, and coal), so that the model will, within a certain time, reach equilibrium. The specific approach entailed adding a 20% step disturbance to each input variable, measuring the response curve of the output variables, and then, based on the response curve, finding the transfer function for the controlled object.

When a 20% step change was added to the amount of hot air and its outlet temperature, the inlet air pressure curve is as shown in Figs. (**2**, **3**).

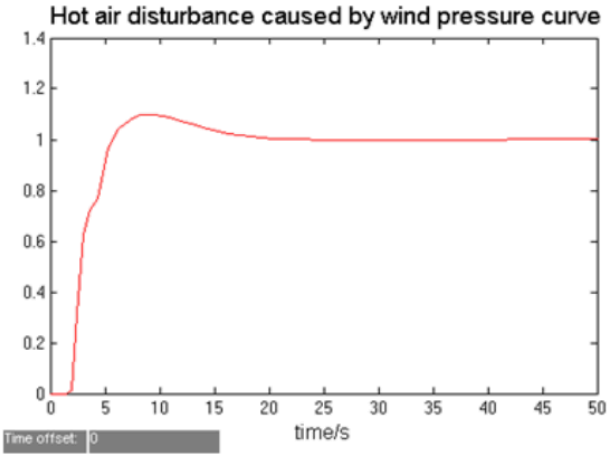

Fig. (2). Hot air disturbance caused by wind pressure.

The results are: $T_1=5, K_1=0.25,\ \tau_1=-2$. Therefore, the object model is $G_{11}=\frac{0.25e^{-2s}}{5s+1}$.

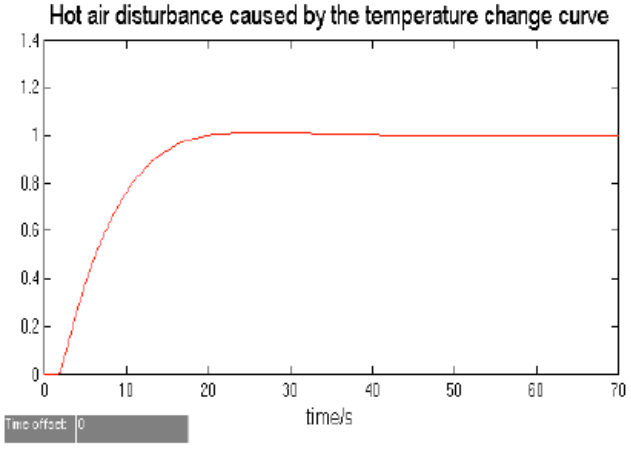

Fig. (3). Hot air disturbance caused by temperature change.

The results are: $T_2=5, K_2=0.8, \tau_2=-2$. Therefore, the object model is

$$G_{12}=\frac{0.8e^{-2s}}{5s+1}.$$

When adding a 20% step change to the amount of cold air and the inlet pressure, the outlet temperature, differential pressure and export curves are as shown in Fig. (**4**).

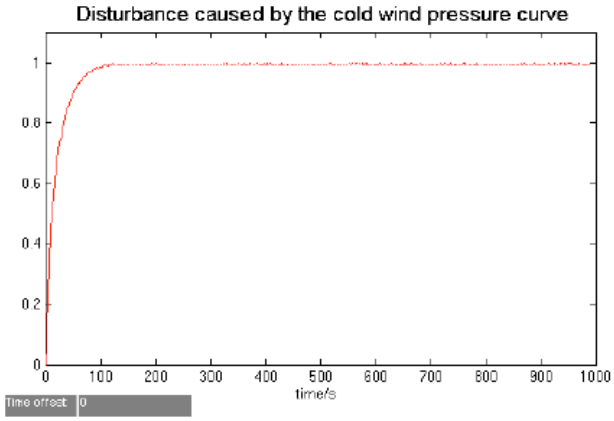

Fig. (4). Disturbance caused by the cold wind pressure.

The results are: $T_3 = 20, K_3 = -0.01, \tau_3 = -5$. Therefore, the object model is

$$G_{21} = \frac{-0.01e^{-5s}}{20s+1}.$$

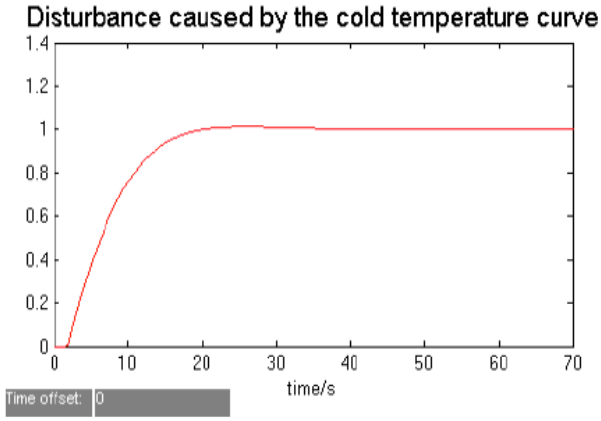

Fig. (5). Disturbance caused by the cold temperature curve.

The results are: $T_4 = 5, K_4 = 0.8, \tau_4 = -2$. Therefore, the object model is $G_{22} = \frac{0.8e^{-2s}}{5s+1}$.

The system transfer function can be written as:

$$\begin{bmatrix} P \\ T \end{bmatrix} = \begin{bmatrix} \frac{0.25e^{-2s}}{5s+1} & \frac{0.8e^{-2s}}{5s+1} \\ \frac{-0.01e^{-5s}}{20s+1} & \frac{0.8e^{-2s}}{5s+1} \end{bmatrix} \begin{bmatrix} U_p \\ U_T \end{bmatrix} \quad (50)$$

5.5. Application of PID-GPC in a Ball-Mill

Three inputs to a ball-mill are: the hot air door opening, cold air door opening, and coal feeder rate of rotation. Three outputs are: the outlet temperature, inlet vacuum, and pressure drop. These three controlled parameters differ significantly in their dynamics, and are strongly coupled. Additionally, the material level and the output temperature of a ball-mill are both characterized by a large time-delay and nonlinearity. All these factors will affect the control of the system [14]. As a ball-mill grinding load is denominated in the variables not subject to the effects of the outlet temperature and negative pressure, the grinding load, and the other two outputs, are fully isolated, thus the 3×3 strongly coupled system is simplified to a dual-input dual-output (TITO) system, so as to reduce system coupling. According to the literature, the PID-GPC parameters are tuned using a trial-and-error method. The key PID-GPC parameters in this work are set as follows: sampling cycle: 1 s, time-domain optimization P = 15, predicted length n = 12, control domain m = 2; control weighted coefficient $\lambda = \begin{bmatrix} 0.46 & 0.90 \end{bmatrix}^T$; softening coefficient $\alpha = \begin{bmatrix} 0.94 & 0.39 \end{bmatrix}^T$; forgetting factor $\lambda_1 = \begin{bmatrix} 1 & 1 \end{bmatrix}^T$; scale factor $P = \begin{bmatrix} 0.8 & 0.0089 \end{bmatrix}^T$; integral coefficients $I = \begin{bmatrix} 0.1 & 0.0062 \end{bmatrix}^T$; and differential coefficient $I = \begin{bmatrix} 0.004 & 0.0054 \end{bmatrix}^T$. These parameters mainly take effect on interference immunity and the robustness of an object, and can be adjusted on-line in the algorithm.

To take a 300 MW large power unit ball-mill pulverizing system running under negative pressure in a power plant in Longshan, Hebei Province as an experimental object, (50) is the transfer function model best describing the system.

Where P ——mill inlet vacuum; T ——mill outlet temperature; U_P ——recirculation door opening degree; and U_T ——hot door opening degree.

To verify the superiority of the PID-GPC algorithm, we compared the method used in this paper with the MAC, GPC and PID control algorithm based on feed-forward compensation decoupling, with the system modeled in (50) as the control object, and compared the proportional integral differential generalized predictive control algorithms proposed in this paper with the PID control algorithm based on the feed-forward compensation decoupling in simulation experiments, and also compared the tracking performance of the system therein.

A GPC controller has parameters that include: the prediction horizon, control horizon, and a weighting factor. These parameters are: the interval for predicting the behaviour of the future output based on a nominal model, the interval for calculating optimal future inputs, and the parameters related to the control input, respectively. The control signals are derived by minimising the performance index on the future control inputs and is then re-calculated receding from their horizons at each sampling time. With these features, the GPC control strategy has been widely accepted.

In MPC, it has been widely recognised that process design plays a key role in process dynamics. Based on the literature [15] on mixed integer dynamic optimisation algorithms, our strategy features high-fidelity process dynamic models, conventional PI control schemes, explicit consideration of structural processes, and control design aspects (such as number of trays, pairing of manipulated and controlled variables) through the introduction of 0–1 variables, and explicit consideration of time-varying disturbances and time-

invariant uncertainties. In the literature [16], a novel methodology for the integrated design (ID) of processes with linear model predictive control (MPC) is addressed, providing, simultaneously, the plant dimensions, the control system parameters and a steady-state working point. The MPC chosen operates over an infinite horizon to guarantee stability and is implemented with a terminal penalty. The ID methodology considers norm-based indices for controllability, as well as robust performance conditions by using a multi-model approach. Others [17] present a new methodology for the simultaneous process flow sheet and control design of dynamic systems under uncertainty using an MPC strategy. The results show that the optimal design obtained by the present method remained feasible and asymptotically stable in the presence of critical facets in the disturbances thereto. Others [18] compute the probability distribution of the worst-case variability of the process variables that determine the dynamic feasibility, or the dynamic performance, of the system under random disturbances. A case study of an actual wastewater treatment industrial plant is presented and used to test the proposed methodology and compare its performance against a quintal design approach and a simultaneous design and control method using conventional PI-based control schemes. In this paper, there are two typical MPC algorithms: GPC and MAC are compared with the algorithm proposed in this paper to verify the dynamic performance of the system.

In this paper, three algorithms were compared: a feed-forward decoupling-based PID control algorithm, GPC algorithm and MAC algorithm. Due to GPC and MAC being two parts of MPC, we can use these algorithms to compare PID-GPC to MPC.

In the simulation experiments, the input is the unit step signal, and the sampling time is 1 s. Fig. (**7**) shows the comparison between the system outputs in the simulation by using the above two control algorithms with the recirculated air volume step inputs. Fig. (**6**) shows the comparison between the system outputs in the simulation by using the aforementioned control algorithms with hot air volume step inputs. Curves a, b, e and g, respectively represent *P*-value outputs for the ball-mill entrance differential pressure at the time of the simulation of the feed-forward compensation decoupling-based PID control algorithm, PID-GPC algorithm, GPC algorithm, and MAC algorithm; curves c, d, f, and h, respectively represent the outlet temperature *T*-value output of the ball-mill at the time of the simulation of the feed-forward compensation decoupling-based PID control algorithm, PID-GPC algorithm, GPC algorithm, and MAC algorithm, respectively.

Fig. (**6**) shows that the *P*-value overshoot of curve a, under feed-forward compensation decoupling-based PID control, is 9.7%, while curve b, under PID-GPC, has no overshoot; the *T*-value overshoot of curve c, under feed-forward compensation decoupling based-PID control, and that of curves d and f, under GPC, curves g and h, under MAC are large.

From those figures that compare system outputs under step inputs of the recirculation air volume and hot air volume, we can see that the PID control, with feed-forward compensation decoupling, is inherently flawed, and is therefore unsuitable for a ball-mill system with large delay and strong coupling [19]. GPC and MAC also have a large time-delay. Instead, the PID-GPC offers good control performance, in which case, the control output overshoot of the ball-mill entrance negative pressure is low, and the adjustment time taken for the outlet temperature to reach a stable value is relatively short.

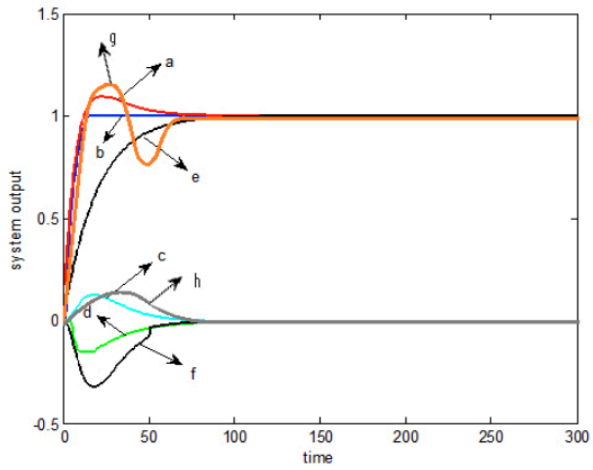

Fig. (6). Comparison of system outputs under recirculating air flow step inputs in the simulation environment.

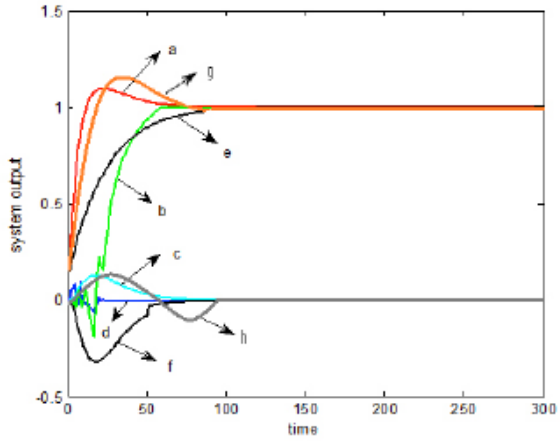

Fig. (7). Comparison of system outputs under hot air volume step inputs in the simulation environment.

To validate further the superiority of the PID-GPC algorithm, we compared the tracking performance of the feed-forward compensation decoupling-based PID control algorithm, GPC algorithm, and MAC algorithm. At t = 200 s, we revised the set value to 2 (as a step signal), and the simulation was then performed over 300 steps.

The simulated results of the performance of the system under system recirculation air volume and hot air volume tracking step inputs are shown in Figs. (**7**, **8**).

Simulation results in Figs. (**8**, **9**) indicate that, compared with the feed-forward decoupling-based PID control algorithm, GPC algorithm, and MAC algorithm, there is no overshoot in the simulation diagram of the system tracking performance under the recycling air flow step inputs in the PID-GPC algorithm, and in the simulation diagram of the

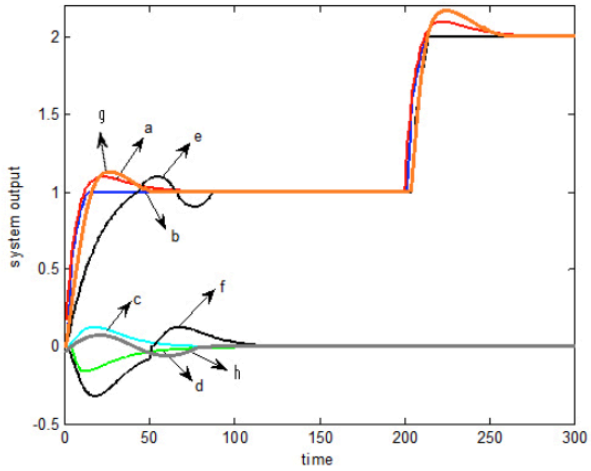

Fig. (8). Comparison of system tracking performance under recirculating air flow step inputs in the simulation environment.

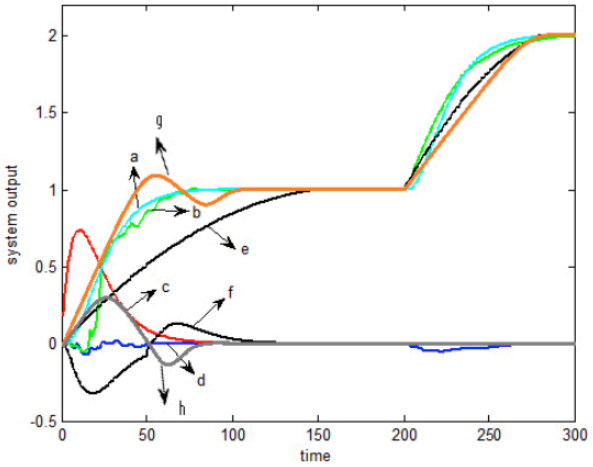

Fig. (9). Comparison of system tracking performance under hot air volume step inputs in the simulation environment.

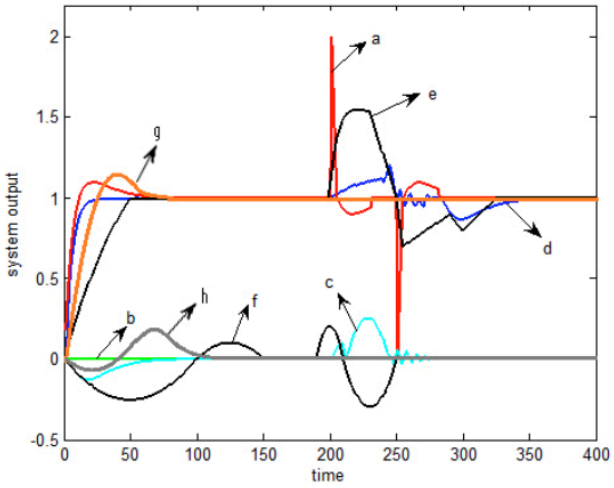

Fig. (10). Comparison of system anti-disturbance performance under recirculating air flow step inputs in the simulation environment.

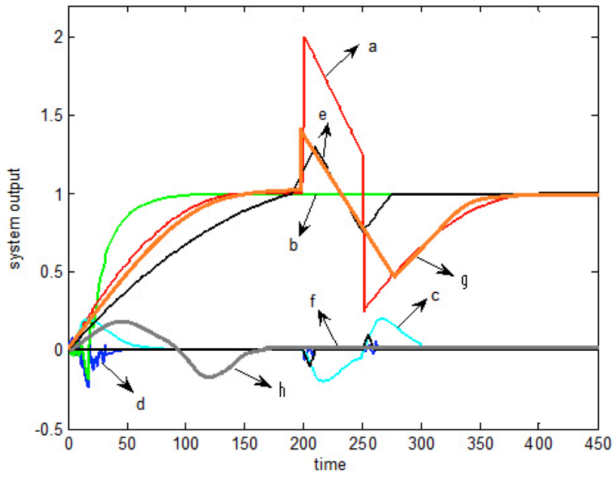

Fig. (11). Comparison of system anti-disturbance performance under hot air volume step inputs in the simulation environment.

system tracking performance under the hot air step inputs, the stabilisation time is short and system step changes can be quickly tracked.

For 200 s ≤ t ≤ 250 s, adding the perturbation amplitude of the pulse to an anti-pulse perturbation characteristic in the system, the simulation results shown in Figs. (**10**, **11**) were obtained.

The simulation results can be seen in Figs. (**10**, **11**): the comparison of the system anti-disturbance performance under hot and cold air volume step inputs in the simulation environment was such that the system showed only slight fluctuations in the PID-GPC algorithm, but based on the feed-forward compensation decoupling PID control algorithm, it was subjected to severe shock, therefore the PID-GPC algorithm conferred a better noise immunity performance.

Due to the lack of lag between the PID controller and process, and the predictive controller being mainly dependent on the control delay time, the control effect seemed to appear in the past. So the controller of the two algorithms combined, can be seen in both speed and overshoot in robustness or response, PID-GPC shows better performance than the other three algorithms see Table **1**. We calculate the four algorithms in the grinding temperature and inlet negative pressure overshoot, rise time, and adjust time, and compared the data see Table **1**.

From Table **1** the overshoot in the PID-GPC algorithm, both in the outlet temperature and inlet pressure control, were less than 20%, and mostly less than feed-forward decoupling PID, GPC, and MAC algorithms; the rise time, except, in order of volume of hot air step input mill inlet pressure is greater than the feed-forward PID and GPC, others are less than those of the feed-forward PID and MAC control algorithms and the the rise was time much shorter, indicating that the PID-GPC algorithm reached a stable state in a shorter time, and was thus suitable for large time delay control systems. In the adjustment time, it reflected the PID-GPC control algorithm and had a response curve which could maintain the status of the error timeously.

Table 1. System control data.

Under recirculating air flow step	**Mill outlet temperature (°C)**			**Mill inlet vacuum (Pa)**		
	Overshoot volume σ (%)	**Rise time t_r (s)**	**Adjusting time t_s (s)**	**Overshoot volume σ (%)**	**Rise time t_r (s)**	**Adjusting time t_s (s)**
GPC	0	24	90	18	23	79
MAC	13.7	19	78	9.8	37	78
feed-forward decoupling-based PID	12.82	20	65	9.7	26	80
PID-GPC	17.48	10	50	0	13	10
Under hot air volume step	**Mill outlet temperature (°C)**			**Mill inlet vacuum (Pa)**		
	Overshoot volume σ (%)	**Rise time t_r (s)**	**Adjusting time t_s (s)**	**Overshoot volume σ (%)**	**Rise time t_r (s)**	**Adjusting time t_s (s)**
GPC	0	99	98	22	18	65
MAC	13	29	76	10	22	100
feed-forward decoupling-based PID	11.8	22	72	9.7	20	56
PID-GPC	5.6	10	25	15.5	55	50

The above analysis of the experimental results shows that:

(1) In terms of overshoot, the PID-GPC algorithm overshoot is lower than the feed-forward PID control overshoot: the overshoots are all less than 20%.

(2) In terms of robustness and interference immunity, the PID-GPC has a short adjustment time and strong adaptability.

(3) In terms of response time, the transition time of the PID-GPC is shorter than that of the GPC algorithm and MAC algorithm, which makes rapid tracking possible. PID-GPC is faster than MPC.

MPC using finite impulse response models, or a finite order step response model, as a process model, without considering the model structure and order in time, can contain a process with a pure time delay; however, it cannot describe an unstable system if stable and on-line model identification is difficult. The advantages of the feedback correction of fusion self-tuning control and predictive control are on-line updating methods, by way of self correction through online model identification and control rules. It can be used for open-loop unstable, non minimum phase and variable delay and it is difficult to control the object, the system of the delay, and the order of the uncertainty has good robustness. The disadvantage of GPC is that it is a multivariable system and the algorithm is relatively difficult to use.

So, MPC has weaknesses in its overshoot, robustness, and interference immunity, or response time, PID-GPC is applicable to MPC in a ball-mill system.

CONCLUSION

Based on the analysis on the working principle behind a double inlet ball-mill, this paper establishes a transfer function mathematical model for a ball-mill, and analyses the ball-mill system by using the generalised predictive self-tuning controller with a proportional and differential structure. Due to the GPC requiring the solution of the Diophantine equation, and matrix inversion, its computational complexity is increased, so it is adapted to lower real-time demands from the system. Findings from the MATLAB™/Simulink modelling and the comparison between PID-GPC and feed-forward decoupling-based PID algorithms: the PID-GPC algorithm was seen to offer good robustness, adaptability, and traceability, which means that it can not only give a fast response and have a small overshoot, but also that it provides an effective solution capable of modeling the characteristics of the ball-mill powder system (*i.e.* large delay and strong coupling). Therefore, the proposed method offers good prospects for wider application.

CONFLICT OF INTEREST

The authors confirm that this article content has no conflict of interest.

ACKNOWLEDGEMENTS

Supported by "Jilin Province Science and Technology Plan Projects", No. 2014020403-0SF.

REFERENCES

[1] D.L. Shi, Y.Y. Li, and D.Y. Zhao, "Fuzzy PID controller Ball Mill Control System Design", *Journal of Northeast Dianli University, Natural Science*, vol. 29, pp. 20-23, 2009.

[2] Y.G. Xi, D.W. Li, and S. Lin, "Model Predictive Control - Current Situation and Challenges", *Automatica Sinica*, vol. 39, pp. 222-236, 2013.

[3] T. Sato, "Design of a GPC-based PID Controller for Controlling a Weigh Feeder", *Control Engineering Practice*, vol. 18, pp. 105-113, 2010.

[4] T. Sato, and A. Inoue, "GPC-based PID Controller Using a Stable Time-varying Proportional Gain", In: *2007 IEEE International Conference on Networking, Sensing and Control*, pp. 536-541, 2007.

[5] T. Yamamoto, T. Yamada, T. Fujii, and H. Hosokawa "Design and Implementation of a GPC-based Auto-tuning PID Controller", In: *IEEE International Conference on Industrial Technology 2006 (ICIT 2006)*, pp. 1920-1924, 2006.

[6] T. Sato, T. Kotani, T. Yamamoto, N. Araki, and Y. Konishi "Design of a Performance-adaptive GPC-PI Control System for Controlling a Weigh Feeder", In: *2012 IEEE International Conference on Control Applications (CCA)*, pp. 521-525, 2012.

[7] C. Pengzhan, and L. Baifen, "Combined PI and GPC for Servo System", In: *2010 International Conference on Computer, Mechatronics, Control and Electronic Engineering*, pp. 254-257, 2010.

[8] P. Ai-Xian, W. Guang-Yi, and H. Dong, "Control of Permanent Magnet Synchronous Motor Based on GPC", In: *4th International Conference on Wireless Communications, Networking and Mobile Computing (WiCOM'08)*, pp. 1-4, 2008.

[9] D.W. Clarke, C. Mohtadi, and P.S. Tuffs, "Generalized predictive control-Part I. The basic algorithm", *Automatica*, vol. 23, pp. 137-148, 1987.

[10] R.R. Li, "Based on Particle Swarm Generalized Predictive Control and Its Application", *Lanzhou Jiaotong University*, vol. 28, pp. 21-23, 2012.

[11] Z. Su, P. Wang, and X. Yu, "Immune Genetic Algorithm-based Adaptive Evidential Model for Estimating Unmeasured Parameter: Estimating levels of coal powder filling in ball mill", *Expert Systems with Applications*, vol. 37, pp. 5246-5258, 2010.

[12] Y. Shi, W. Guo, W. Wang, "PID- GPC in Superheated Temperature Control System", *Computer Engineering*, vol. 37, pp. 251-253, 2009.

[13] L.F. Sun, L. Dan, and J.M. Sun, "Modeling of Ball Mill Pulverizing System and Research of Support Vector Machine Generalized Inverse with Internal Model Control", *Information Technology Journal*, vol. 12, pp. 8405-8411, 2013.

[14] W.H. Tao, T.Y. Chai, and H. Yue, "Ball mill Model and Simulation of Dynamic Parameters", *Journal of System Simulation*, vol. 16, pp. 778-780, 2004.

[15] V. Sakizlis, J.D. Perkins, and E.N. Pistikopoulos. "Recent advances in optimization-based simultaneous process and control design". *Computers & Chemical Engineering*, vol. 28, pp. 2069-2086, 2004.

[16] M. Francisco, P. Vega, H. Álvarez. "Robust Integrated Design of processes with terminal penalty model predictive controllers". *Chemical Engineering Research & Design*, vol. 89, pp. 1011-1024, 2011

[17] K.B. Sanchezsanchez, and L.A. Ricardezsandoval, "Simultaneous Design and Control under Uncertainty Using Model Predictive Control", *Industrial & Engineering Chemistry Research*, vol. 52, pp. 4815-4833, 2013

[18] S.S. Bahakim, and L.A. Ricardez-Sandoval, "Simultaneous design and MPC-based control for dynamic systems under uncertainty: A stochastic approach", *Computers & Chemical Engineering*, vol. 63, pp. 66-81, 2014.

[19] L.J. Chen, Z.X. Zhou, and L.L. Zhao, "The application of advanced control strategy in thermal control of power plant", *Journal of Northeast Dianli University, Natural Science, Natural Science*, vol. 1, pp. 25-29, 2009.

Received: December 15, 2014 Revised: January 04, 2015 Accepted: February 25, 2015